AFRL-RV-PS-
TR-2014-0059

AFRL-RV-PS-
TR-2014-0059

GROWTH AND DEFECT CHARACTERIZATION OF QUANTUM DOT-EMBEDDED III-V SEMICONDUCTORS FOR ADVANCED SPACE PHOTOVOLTAICS

Steve Ringel, et al.

Ohio State University
The Office Of Sponsored Programs
1960 Kenny Rd
Columbus, OH 43210-1016

15 May 2014

Final Report

AIR FORCE RESEARCH LABORATORY
Space Vehicles Directorate
3550 Aberdeen Ave SE
AIR FORCE MATERIEL COMMAND
KIRTLAND AIR FORCE BASE, NM 87117-5776

DTIC COPY
NOTICE AND SIGNATURE PAGE

This report is the result of contracted fundamental research deemed exempt from public affairs security and policy review in accordance with SAF/AQR memorandum dated 10 Dec 08 and AFRL/CA policy clarification memorandum dated 16 Jan 09. This report is available to the general public, including foreign nationals. Copies may be obtained from the Defense Technical Information Center (DTIC) (http://www.dtic.mil).

AFRL-RV-PS-TR-2014-0059 HAS BEEN REVIEWED AND IS APPROVED FOR PUBLICATION IN ACCORDANCE WITH ASSIGNED DISTRIBUTION STATEMENT.

//SIGNED//
DAVID WILT
Program Manager

//SIGNED//
PAUL HAUSGEN
Technical Advisor, Spacecraft Component Technology Branch

//SIGNED//
BENJAMIN M. COOK, Lt Col, USAF
Deputy Chief, Spacecraft Technology Division
Space Vehicles Directorate

Approved for Public Release; distribution is unlimited.

REPORT DOCUMENTATION PAGE

Form Approved
OMB No. 0704-0188

1. REPORT DATE *(DD-MM-YYYY)*	**2. REPORT TYPE**	**3. DATES COVERED** *(From - To)*
15-05-2014	Final Report	24 May 2012 – 06 Mar 2014

4. TITLE AND SUBTITLE
Growth and Defect Characterization of Quantum Dot-Embedded III-V Semiconductors for Advanced Space Photovoltaics

5a. CONTRACT NUMBER
FA9453-12-1-0219

5b. GRANT NUMBER

5c. PROGRAM ELEMENT NUMBER
62601F

6. AUTHOR(S)
Steve Ringel, Tyler Grassman, and John P. Saving

5d. PROJECT NUMBER
8809

5e. TASK NUMBER
PPM00017645

5f. WORK UNIT NUMBER
EF008953

7. PERFORMING ORGANIZATION NAME(S) AND ADDRESS(ES)
Ohio State University
The Office Of Sponsored Programs
1960 Kenny Rd
Columbus, OH 43210-1016

8. PERFORMING ORGANIZATION REPORT NUMBER

9. SPONSORING / MONITORING AGENCY NAME(S) AND ADDRESS(ES)
Air Force Research Laboratory
Space Vehicles Directorate
3550 Aberdeen Ave., SE
Kirtland AFB, NM 87117-5776

10. SPONSOR/MONITOR'S ACRONYM(S)
AFRL/RVSV

11. SPONSOR/MONITOR'S REPORT NUMBER(S)
AFRL-RV-PS-TR-2014-0059

12. DISTRIBUTION / AVAILABILITY STATEMENT
Approved for Public Release; distribution is unlimited.

13. SUPPLEMENTARY NOTES

14. ABSTRACT
A number of different QD/host materials systems were investigated via molecular beam epitaxy (MBE), ranging from the well-known lattice-matched host materials – InAs/GaAs, $Ga_{0.50}In_{0.50}As$/GaAs, InP/$Ga_{0.51}In_{0.49}P$, and even InAs/$Ga_{0.51}In_{0.49}P$ (which has actually seen very little investigation) – to metamorphic host materials systems that have not previously been studied – $Ga_{0.55}In_{0.45}As$/$GaAs_{0.90}P_{0.10}$ and InP/$Ga_{0.56}In_{0.44}P$. From these exploratory materials efforts, two main conclusions were made: (1) QD/host materials compatibility have a major impact on ease of controlling the morphology and quality of the heterogeneous system, and (2) the use of metamorphic substrates appears to provide, in addition to better control over the QD/host electronic structure by giving a choice of materials, an additional parameter for control over QD size and density beyond what misfit and deposition conditions can provide, which could be useful in the future development of intermediate band solar cell (IBSC) devices. Defect spectroscopy was also performed on OMVPE-grown InAs/GaAs QD-embedded solar cells. A large increase in mid-gap trap density surrounding the embedded QDs was found and points to a potentially important performance degradation mechanism, and provides a target for future comparisons with MBE-grown QD/host systems.

15. SUBJECT TERMS
solar cell calibration, high altitude solar cell calibration, high altitude balloon solar cell calibration, III-V compound semiconductors, solar cells, intermediate band, quantum dots, metamorphic III-V semiconductors, virtual substrates, defect spectroscopy, molecular beam epitaxy

16. SECURITY CLASSIFICATION OF:			**17. LIMITATION OF ABSTRACT**	**18. NUMBER OF PAGES**	**19a. NAME OF RESPONSIBLE PERSON**
a. REPORT	**b. ABSTRACT**	**c. THIS PAGE**			David Wilt
U	U	U	Unlimited	28	**19b. TELEPHONE NUMBER** *(include area code)*

(This page intentionally left blank)

TABLE OF CONTENTS

LIST OF FIGURES

PREFACE

The following is a final progress report for Air Force Research Laboratory project FA9453-12-1-0219. The objectives of this project were to explore the growth of epitaxial quantum dots (QDs) within different hosts materials – and specifically metamorphic (i.e. fully-relaxed lattice-mismatched) materials – to enable the transition toward wider-gap host materials that are more in-line with intermediate band solar cell type devices, as well as gain additional understanding into the defects created by embedding QDs within photovoltaic (PV) materials through characterization of QD/host structures and comparison between growth methodologies. This project was undertaken within the group of PIs T. Grassman and S. Ringel at the Ohio State University, with the majority of the laboratory work performed by Dr. T. Grassman. The report authors wish to acknowledge additional laboratory efforts by Dr. D. Cardwell, Dr. A. Arehart, and W. Sun. We would also like to acknowledge the group of Dr. S. Hubbard and Dr. D. Forbes of the Rochester Institute of Technology and the National Aeronautics and Space Administration's Glenn Research Laboratory for supplying solar cell structures for defect spectroscopy analysis.

ACKNOWLEDGMENTS

This material is based on research sponsored by Air Force Research Laboratory under agreement number FA9453-12-1-0219. The U.S. Government is authorized to reproduce and distribute reprints for Governmental purposes notwithstanding any copyright notation thereon.

DISCLAIMER

The views and conclusions contained herein are those of the authors and should not be interpreted as necessarily representing the official policies or endorsements, either expressed or implied, of Air Force Research Laboratory or the U.S. Government.

1 SUMMARY

Achieving maximum solar cell efficiency requires nearly perfect use of the solar spectrum with respect to optical absorption, coupled with nearly ideal electronic transport properties, so that photogenerated carrier collection efficiency across the entire spectrum can be maximized. For space solar cell technologies, the III-V multijunction (MJ) concept has been the leading approach to date [1], but even this method has its limits in terms of achieving ultimate efficiencies due to a number of practical limitations. Hence, in parallel to the continued advance of MJ technologies and their current day implementation, there is now great interest for the next generation of space photovoltaic (PV) technologies to exploit the physics of quantum dot (QD) enhanced PV structures that have the potential to make game-changing advances for space PV power. While the experimental validation of the many QD-enhanced PV concepts is still in the very early stages of exploration, key to their success will be a total understanding of the defect modes that form as a result of QD incorporation. This, in turn, will depend on growth method, growth conditions, choice of QD and host materials, control of lattice mismatch and strain, etc. Therefore, the goals of this effort were to explore the growth of epitaxial QDs within different hosts materials – and specifically metamorphic (i.e. fully-relaxed lattice-mismatched) materials – moving toward wider-gap hosts and to gain additional understanding into the defects created by embedding QDs within PV materials through characterization of QD/host structures and comparison between growth methodologies.

In the course of this project we investigated a number of different QD/host materials systems, ranging from the well-known lattice-matched host materials – InAs/GaAs, $Ga_{0.50}In_{0.50}As$/GaAs, InP/$Ga_{0.51}In_{0.49}P$, and even InAs/$Ga_{0.51}In_{0.49}P$ (which has actually seen very little investigation) – to metamorphic host materials systems that have not previously been studied – $Ga_{0.55}In_{0.45}As$/$GaAs_{0.90}P_{0.10}$ and InP/$Ga_{0.56}In_{0.44}P$. While the materials exploratory effort yielded a number of interesting results, there were a few key conclusions made from them. Perhaps the most important is that the use of metamorphic substrates appears to provide, in addition to better control over the QD/host electronic structure by giving a choice of materials, an additional parameter for control over QD size and density beyond what misfit and deposition conditions can provide, which could be useful in the future development of IBSC devices. Of course, the application of such flexibility is still subject to restrictions with respect to materials compatibility, as evidenced by the results of the InAs/GaInP efforts, which suggest that some kind of work-around may be needed to enable the use of GaInP as a host material, or that a different wide-gap host material altogether (GaAsP) may provide a more reliable solution. Both approaches warrant further investigation.

The defect spectroscopy work provided some insight into electronic defects in QD-embedded materials, specifically with respect to the well-known InAs/GaAs QD/host system, as grown by organometallic vapor phase epitaxy (OMVPE). Here, the large increase in mid-gap trap density surround the embedded QDs points to a potentially important performance degradation mechanism in this system. Future comparisons against molecular beam epitaxy (MBE) grown samples, coupled with detailed structural characterization, will further enhance our understanding of these defects. Extension of this study to other QD/host materials, especially the "new" metamorphic systems, should be strongly considered.

2 INTRODUCTION

Achieving maximum solar cell efficiency requires nearly perfect use of the solar spectrum with respect to optical absorption, coupled with nearly ideal electronic transport properties, so that photogenerated carrier collection efficiency across the entire spectrum can be maximized. This double requirement, of ideal spectral utilization and high electronic transport quality, has arguably been the defining challenge for every photovoltaics (PV) technology. For space solar cell technologies, the III-V multijunction (MJ) concept has been the leading approach to date [1], but even this method has its limits in terms of achieving ultimate efficiencies due to a number of practical limitations: the number of vertically-stacked junctions that can realistically maintain current-matching over the lifetime of a cell array; achieving ideal spectral splitting through metamorphic engineering over large ranges of lattice mismatch; complexities that are exacerbated by space and radiation environments. Hence, in parallel to the continued advance of MJ technologies and their current day implementation, there is now great interest for the next generation of space PV technologies to exploit the physics of quantum dot (QD) enhanced PV structures that have the potential to make game-changing advances for space PV power.

The use of QDs in PV devices is theoretically compelling for a number of reasons: incorporation into MJ cells to improve radiation resistance and maintain current matching over the array lifecycle [2]; extension of the spectral sensitivity of subcells without the addition of new junctions [3]; and the possibility of creating the so-called intermediate band solar cell (IBSC) in which theoretical efficiencies that exceed ideal MJ cells have been predicted, without the need for more than a single *p-n* junction [4]. Moreover, advanced device concepts, such as the *nipi* cell architecture [5], which directly addresses the problem of photogenerated carrier localization and recombination through the use of a *n-i-p-i* "doping superlattice" that separates photogenerated electrons and holes into separate transport channels, would greatly benefit from QD incorporation to expand the spectral utilization by reducing thermalization losses in the single band gap design.

Of course the experimental validation of the many QD-enhanced PV concepts is in the very early stages of exploration. Key to their success will be a total understanding of the defect modes that form as a result of QD incorporation, which in turn depends on growth method, growth conditions, choice of QD and host materials, control of lattice mismatch and strain, etc. To date, such defect formation and mitigation issues have not been well explored, if even considered at all. The aim of the project was to investigate these issues in two QD/host materials families of great interest for space PV: InAs/GaAs and GaInAs/GaInP. Molecular beam epitaxy (MBE) was targeted as the main synthesis method to be used to create these structures, complementing the organometallic vapor phase epitaxy (OMVPE) work done by the Rochester Institute of Technology (RIT) group led by S. Hubbard on InAs/GaAs.

The goal of this effort was effectively two-fold. First was to explore the growth of epitaxial QDs within different hosts materials, and specifically metamorphic (i.e. fully-relaxed lattice-mismatched) materials, moving toward wider-gap hosts, and thus closer to the ideal values for IBSC designs. Second was to gain additional understanding into the defects created by embedding QDs within PV materials through characterization of QD/host structures and comparison between growth methodologies (MBE vs. OMVPE).

3 METHODS, ASSUMPTIONS, AND PROCEDURES

All quantum dot (QD) growths reported here were performed in a Varian Gen II solid source molecular beam epitaxy (MBE) chamber with valved P_2 and As_2 cracker sources; the one exception are the organometallic vapor phase epitaxy (OMVPE) samples produced by the Hubbard group for defect spectroscopy characterization. Idle background pressure in the ultra-high vacuum (UHV) MBE growth chamber was $< 2\times10^{-10}$ Torr. Temperatures were measured via a combination of substrate heater mounted thermocouple and infrared pyrometry; the latter was calibrated with the Al-Si eutectic melt and GaAs oxide desorption temperatures. In-situ monitoring of the growths was performed via reflection high-energy electron diffraction (RHEED). For the case of QD growths, the RHEED is used to infer QD nucleation by the transition of the streaky diffraction pattern (indicating a smooth, well-ordered surface) into a spotty pattern (indicating surface roughness on a nanometer length-scale). Inversely, QD encapsulation can be inferred by the transition from a spotty pattern back to a streaky pattern.

All growths were performed on GaAs(100) substrates intentionally misoriented 6° toward the nearest (111)A. Metamorphic virtual substrates were produced by way of tensile-strained step-graded $GaAs_yP_{1-y}$ buffers. Threading dislocation density (TDD) for the $GaAs_{0.90}P_{0.10}$/GaAs virtual substrates was measured at $\sim1\times10^{6}$ cm^{-2} via cathodoluminescence (CL). For all growths the host/matrix layers were doped n-type (Si) to $N_D = 1\times10^{17}$ cm^{-3}, while the QDs were not intentionally doped.

Sample analysis included atomic force microscopy (AFM) for surface morphology characterization, high-resolution triple-axis X-ray diffraction (XRD) reciprocal space mapping (RSM) for structural analysis (composition, strain, crystal quality), and photoluminescence (PL) for characterization of optical properties. Electronic defect characterization was performed on fabricated diode structures via deep level transient spectroscopy (DLTS). DLTS measurements were taken over a range of reverse bias values to provide effective depth resolution by controlling the edge of the space-charge region, taking care (in the case of the QD-embedded structure) to ensure that the depletion tails were sufficiently above or behind the region of interest to avoid inaccuracies related to the lambda effect. A 0.0 V, 10.0 msec pulse was used in between transient measurements in order to refill the previously-emptied traps. Measurements were performed over a temperature range of 80 K to 400 K to enable extraction of trap energy and capture cross section. Data was taken and analyzed using a boxcar method via a custom-built computer-controlled DLTS system that includes a function generator to provide trap filling and a 1 MHz operation capacitance meter, along with a digital oscilloscope for averaging and recording the capacitance transients. This instrumentation is capable of observing trap densities down into the $\sim10^{11}$ cm^{-3} range, depending upon the background doping of the material under investigation.

4 RESULTS AND DISCUSSION

Note that the following subsections are presented in the same order as the original proposal statement of work (SOW), but were not necessarily investigated in the same chronological order.

4.1 GaInAs QDs with GaAsP Host

This effort followed and expanded upon previous work on the growth of epitaxial GaInAs QDs on and within a metamorphic GaAsP matrix. Where previous work demonstrated single- and multi-layer $Ga_{0.67}In_{0.33}As$ QD growth on both compressive- and tensile-graded $GaAs_{0.90}P_{0.10}$ [6], this effort focused on increasing the In content to 45%, or $Ga_{0.55}In_{0.45}As$, in order to equal the lattice mismatch of the well-known $Ga_{0.50}In_{0.50}As$/GaAs QD system, which we have also previously investigated (unpublished). While this work was not specifically called for within this project's SOW, it is within the purview of the overall metamorphic (Ga)InAs/GaInP QD effort with respect to the better understanding of metamorphic quantum dots at this lattice constant and with the same degree of lattice mismatch. Additionally, it is also within the range of interest for targeted QD compositions, but using a host material that is not prone to strain-induced materials instabilities.

The initial focus here was toward the investigation of the nucleation of $Ga_{0.55}In_{0.45}As$ QDs grown on metamorphic $GaAs_{0.90}P_{0.10}$ host material. To this end, Figure 1 presents a set of AFM images of single-layer $Ga_{0.55}In_{0.45}As$ QDs grown on tensile-graded $GaAs_{0.90}P_{0.10}$/$GaAs_yP_{1-y}$/GaAs virtual substrates (with a threading dislocation density of ~$1x10^6$ cm^{-2}) using a range of $Ga_{0.55}In_{0.45}As$ coverages, starting slightly above the expected QD critical thickness, from 3.9 – 4.6 monolayers (ML). Round dots, with increasing density at increasing deposited GaInAs, are seen. These results are consistent with previous work on $Ga_{0.50}In_{0.50}As$/GaAs QDs, which indicates that the relatively low dislocation density in the terminal virtual substrate layer did not have a significant effect on the dot formation. Of interest here is the relatively high degree of uniformity, especially in the highest coverage, with on average QD dimension (height × diameter) of approximately 5 nm × 35 nm and QD number density ranging from 2–$6×10^{10}$ cm^{-2}.

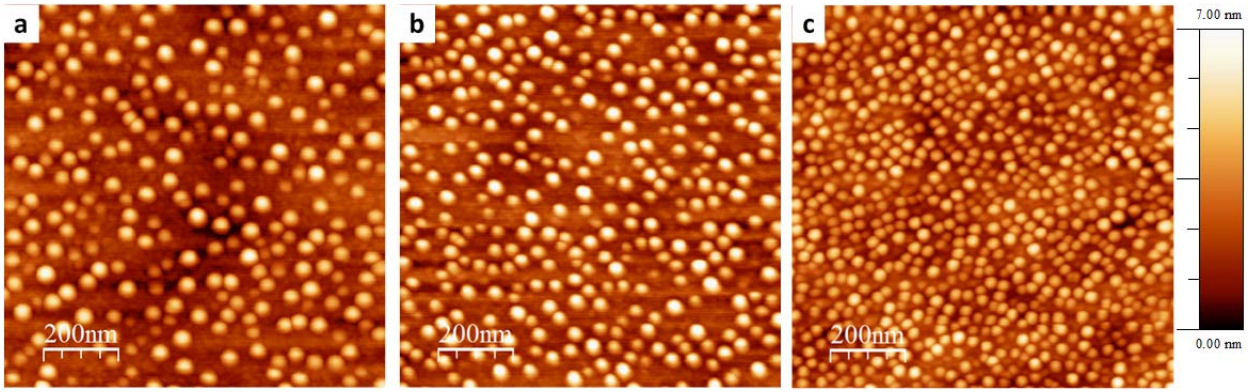

Figure 1. AFM images of single-layer $Ga_{0.55}In_{0.45}As$ QD growths on $GaAs_{0.90}P_{0.10}$ virtual substrates for a range of $Ga_{0.55}In_{0.45}As$ deposition thickness: (a) 3.9 ML, (b) 4.2 ML, and (c) 4.6 ML.

Figure 2 displays AFM and XRD-RSM data from a 20 period $Ga_{0.55}In_{0.45}As/GaAs_{0.90}P_{0.10}$ multi-layer QD growth using a $Ga_{0.55}In_{0.45}As$ deposition thickness of 4.2 ML per QD layer (same as in Fig. 1b), with a final 21st QD surface layer for topographical analysis; no additional strain compensation was utilized. The resultant QD density here, 4.4×10^{10} cm^{-2}, actually ended up slightly higher than that of Fig. 1b, which could be a result of slight growth condition variation or due to some kind of strain effect. The XRD-RSM in Fig. 2b indicates sharp interfaces, with an expected build-up of compressive strain due to the lack of any strain-compensating/balancing tensile layers.

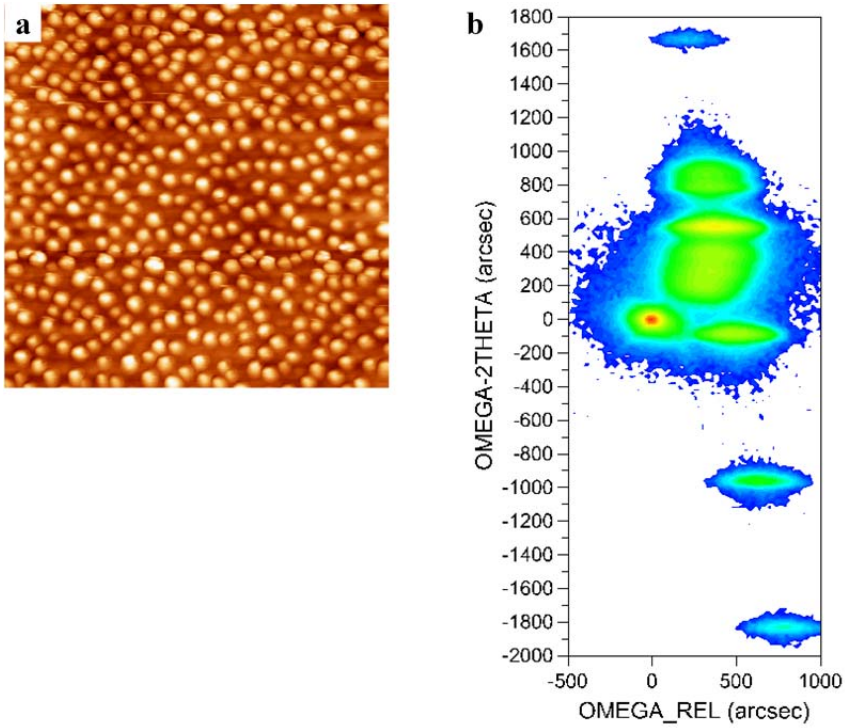

Figure 2. (a) AFM and (b) XRD-RSM from an MBE-grown 20-period multilayer $Ga_{0.55}In_{0.45}As/GaAs_{0.90}P_{0.10}$ structure.

Figure 3 presents a comparison of multilayer QD/host samples for "lattice-matched" $Ga_{0.50}In_{0.50}As/GaAs$ and metamorphic $Ga_{0.55}In_{0.45}As/GaAs_{0.90}P_{0.10}$, which possess equal levels of compressive strain, 3.6% misfit. The QD layers were produced using depositions of 4.2 ML and a terminal QD capping layer was grown to enable topological analysis. No intentional strain compensation was provided in these structures. Full-width at half-max is noted for each QD PL emission peak to demonstrate QD size uniformity, and substrate/host emission peaks are also labeled. Also note that the $Ga_{0.50}In_{0.50}As/GaAs$ data is from a 60-period structure, which provided the narrowest PL peak width and highest degree of self-assembly order versus similar 20- and 40-period structures (not shown), while the $Ga_{0.55}In_{0.45}As/GaAs_{0.90}P_{0.10}$ data is from a 20-period structure (higher-period structures have not been grown). Despite the equal lattice mismatch, the very similar compositions, and effectively identical growth conditions – temperatures, deposition rates, group-V vs. group-III (hereafter denoted V:III) beam flux ratios, substrate offcut – for both systems, clear differences between the two cases can be seen. The $Ga_{0.55}In_{0.45}As/GaAs_{0.90}P_{0.10}$ QDs are found to be smaller (height × diameter of ~5×35 nm^2) than the $Ga_{0.50}In_{0.50}As/GaAs$ case (~8×40 nm^2), and three times greater density (4.4×10^{10} cm^{-2} vs.

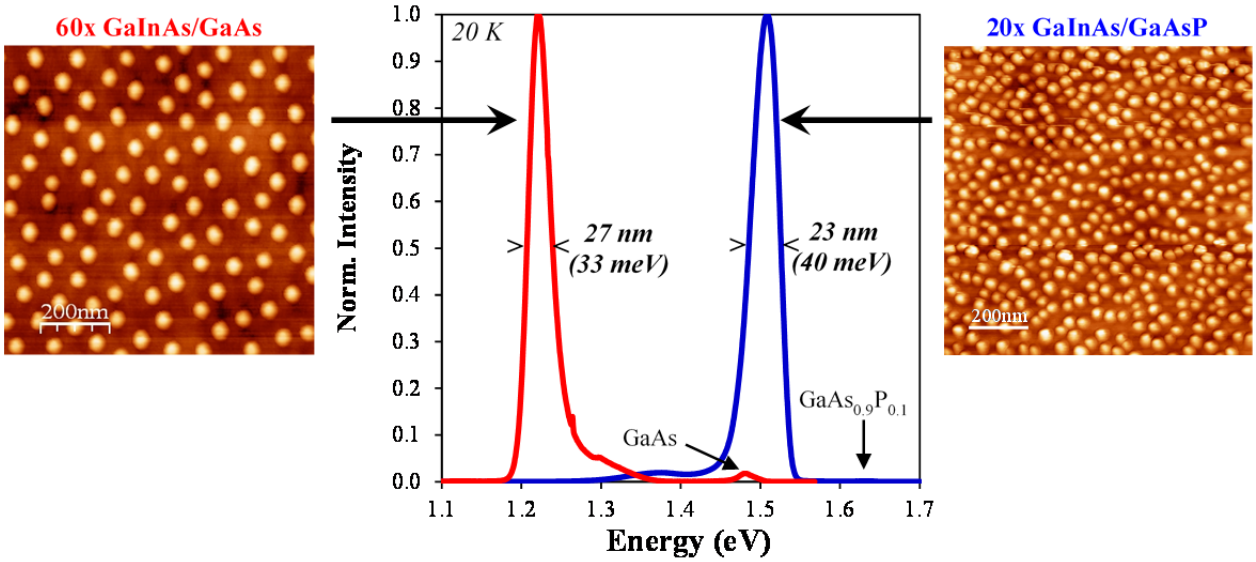

Figure 3. AFM images and low-temperature PL spectra for $Ga_{0.50}In_{0.50}As$/GaAs (red) and $Ga_{0.55}In_{0.45}As/GaAs_{0.90}P_{0.10}$ (blue) QD multilayer structures.

1.3×10^{10} cm^{-2}); note that while the QDs in the $Ga_{0.50}In_{0.50}As$/GaAs case do appear slightly ellipsoidal in the AFM image provided, this is actually due to uncorrected drift in the AFM at the time of measurement. Additionally, the $Ga_{0.50}In_{0.50}As$/GaAs QDs show a relatively high degree of hexagonal self-assembly, while the $Ga_{0.55}In_{0.45}As/GaAs_{0.90}P_{0.10}$ QDs do not to appear to possess any such long-range ordering.

The stronger blue shift of the metamorphic $Ga_{0.55}In_{0.45}As/GaAs_{0.90}P_{0.10}$ ($\geq$ 600 meV) versus that of the $Ga_{0.50}In_{0.50}As$/GaAs structure (380 meV), given the comparatively small changes in bulk band gaps of the QD and host materials (+57 meV for $Ga_{0.50}In_{0.50}As$-to-$Ga_{0.55}In_{0.45}As$, +118 meV for GaAs-to-$GaAs_{0.90}P_{0.10}$), is consistent with the reduction in QD size observed via AFM. The peak width from the 20x $Ga_{0.55}In_{0.45}As/GaAs_{0.90}P_{0.10}$ structure (40 meV) is on par with the well-ordered 60x $Ga_{0.50}In_{0.50}As$/GaAs structure (33 meV), but significantly narrower than 40x or 20x $Ga_{0.50}In_{0.50}As$/GaAs structures (not shown).

4.2 InAs QDs with GaInP Host by MBE

This task focused on the growth of (Ga)InAs QDs grown using a metamorphic Ga-rich GaInP host/matrix. Specifically, the proposal was to utilize ~2.0 eV $Ga_{0.56}In_{0.44}P$, grown lattice-matched to $GaAs_{0.90}P_{0.10}/GaAs_yP_{1-y}$/GaAs virtual substrates (step-graded buffers). This task was anticipated to be particularly challenging due to the well-known phase instability issues in the $Ga_{1-x}In_xP$ alloy system – namely the tendency for phase separation into In- and Ga-rich phases – which are significantly exacerbated by excess interfacial strain (i.e. lattice-mismatch/misfit) [7,8]. In the case of the metamorphic $Ga_{0.56}In_{0.44}P$ host material, the source of potentially problematic strain is not only the QDs themselves (highly localized strain fields), but also any residual strain coming from the $GaAs_yP_{1-y}$ buffer (delocalized strain field). As such, it was expected that highly-optimized growth conditions, coupled with a detailed strain-balancing approach, would be necessary to achieve truly high-quality QD incorporation. That is, of course, provided that controllable, reproducible, uniform QD nucleation and growth itself is actually achievable.

In order to reduce the number of potential strain-related issues in the early stage research, we decided to begin by looking at the more "standard" $Ga_{0.51}In_{0.49}P$ (E_g ~ 1.9 eV), which is lattice-matched to GaAs. Initial work began by investigating InAs QD nucleation and growth on this host material; note that this provides a QD/host lattice mismatch of 7.2%. Figure 4 presents AFM images taken from two such growths, wherein InAs QDs were deposited using conditions that were previously verified as being successful for growth on GaAs and GaAsP host materials. In these two example growths, total InAs deposition thicknesses of 1.5 ML and 2.0 ML were used, with the prior being just above the InAs/GaAs QD critical nucleation thickness. The immediate obvious observation in these images is the stark difference between these QD surface morphologies versus those of similarly situated (Ga)InAs/GaAs(P) QD/host systems, such as shown previously in Figs. 1-3. Whereas the GaAs(P) host systems showed good QD uniformity and nucleation reproducibility, the InAs/GaInP system shows massive non-uniformity, with sizes ranging from very small, just-nucleated dots to large, coalesced "blobs," even at InAs depositions lower than those for the GaAs(P) host samples.

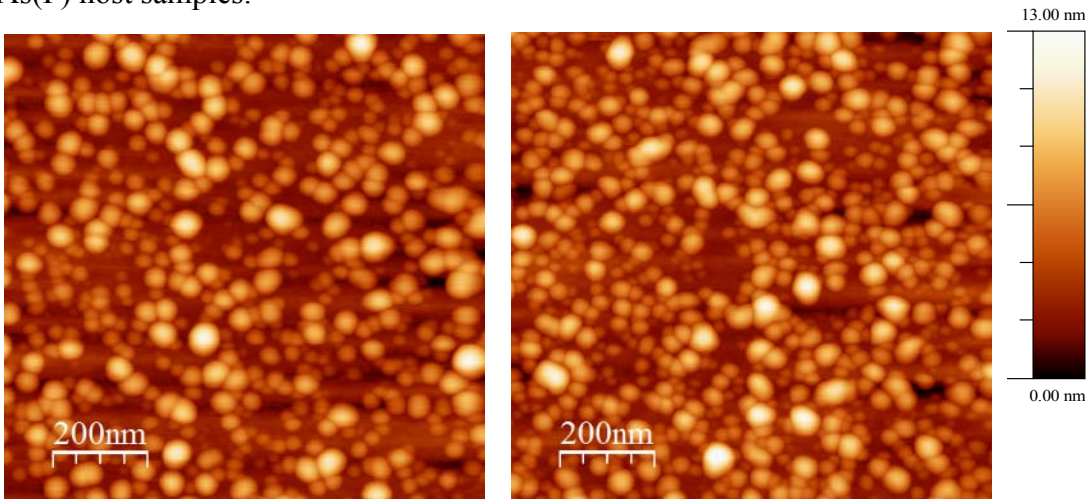

Figure 4. AFM images of (a) 1.5 ML and (b) 2.0 ML InAs QDs growth on nominally lattice-matched GaInP/GaAs.

To further explore the impact of this non-ideal, non-uniform QD nucleation morphology, we grew a few InAs/$Ga_{0.51}In_{0.49}P$ QD/host multiplayer structures. AFM from two such structures are shown in Figure 5. Both growths shown here used identical InAs growth conditions and depositions of 1.5 ML, with a five-period QD/host structure plus a final surface QD layer; the structure shown in (b) utilized a GaInP encapsulation growth rate twice that of (a) – 0.24 ML/sec versus 0.12 ML/sec – to investigate whether a faster encapsulation rate might be able to help overcome the assumed phase instability problems exhibited by (a). However, in both cases, it was observed that the typical "spotty" RHEED patterns created by QD formation no longer appeared after only the second period, suggesting that the originally high (7.2%) strain conditions were no longer conducive to yield QD nucleation. Indeed, as evidenced by the rough, pitted surface morphology, it appears as though the GaInP encapsulation layers most likely are undergoing massive destabilization and resulting phase separation due to the highly non-uniform strain distribution, most likely coming from the large coalesced QDs; the density of the deep pits is roughly equal to the density of large, coalesced dots.

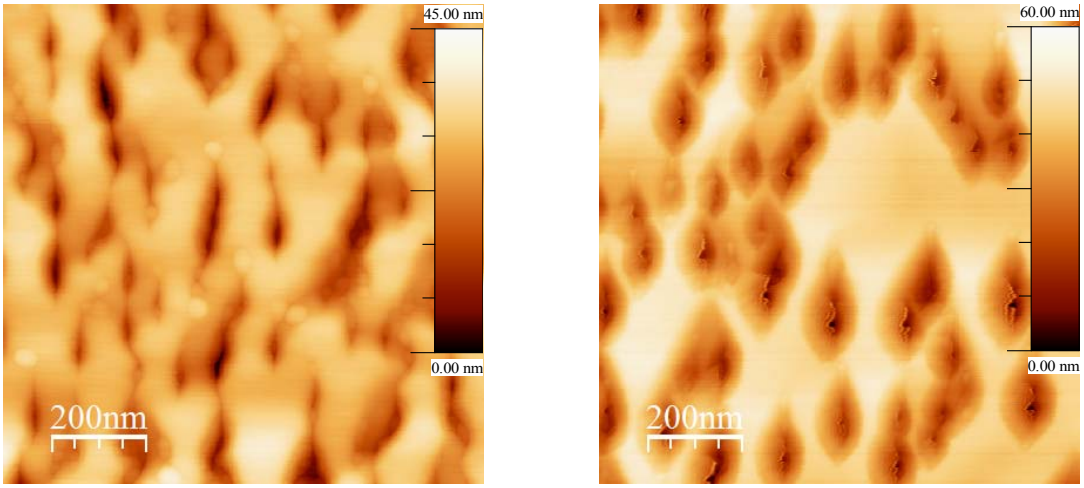

(a) **(b)**

Figure 5. AFM images from five-period InAs/$Ga_{0.51}In_{0.49}P$ QD/host multilayer growths, with $Ga_{0.51}In_{0.49}P$ encapsulation layers grown at (a) 0.12 ML/sec and (b) 0.24 ML/sec.

4.3 InP QDs with GaInP Host

Given the results of the InAs/GaInP QD/host structure exploration described above, and to further investigate the issue of possible In accumulation, we undertook a study concerning the growth of InP QDs with a GaInP host, using both lattice-matched $Ga_{0.51}In_{0.49}P$ and metamorphic $Ga_{0.56}In_{0.44}P$, with nominal lattice mismatches (strain) of 3.8% and 4.2%, respectively. There is sufficient literature reports of successful InP/$Ga_{0.51}In_{0.49}P$ growth [9,10], so the initial effort was to reproduce such results within our MBE system to enable a shift to the metamorphic host, for which there are no literature reports (on metamorphic GaInP, anyway). Initial InP QD nucleation (on $Ga_{0.51}In_{0.49}P$) test growths informed us that very large P_2 overpressure values were needed to achieve controllable, uniform QD nucleation and growth, most likely due to the high diffusivity of In and a possibly higher kinetic barrier to reaction than for the InAs dots. After finding reasonable nucleation conditions, we proceeded to grow multilayer test structures to determine the stability of the GaInP.

Figure 6 presents AFM images from a 10-period multilayer InP/$Ga_{0.51}In_{0.49}P$ structure. In stark contrast to the InAs/$Ga_{0.51}In_{0.49}P$ case, which effectively resulted in disastrous decomposition of the $Ga_{0.51}In_{0.49}P$ host, the structures here show well-formed, uniform, ordered QDs, even after 10 periods, clearly indicating a huge difference in either the QD/host interaction of the surface chemistry during growth, or both. The QDs here show very regular, long-range, square-packed ordering, consistent with literature reports. There are slight signs of some small-scale pitting indicating that the GaInP host may be starting to become unstable due to the strain build-up, but nowhere near as bad as in the InAs/GaInP case. In this case, given the high degree of uniformity, some kind of strain-balancing layers would most likely be successful, whereas in the InAs case the large non-uniformity would make strain compensation difficult.

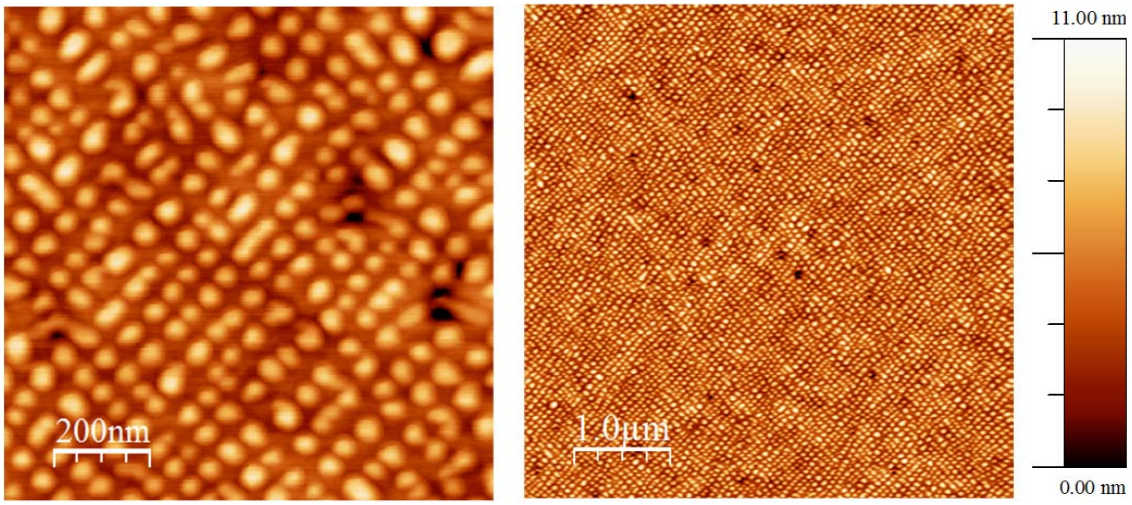

Figure 6. AFM images from an example 10-period multilayer InP/ $Ga_{0.51}In_{0.49}P$ QD/host layer growth taken at two different length scales. InP depositions of 4.2 ML were used.

With this initial demonstration of capability on lattice-matched $Ga_{0.51}In_{0.49}P$, we moved to the metamorphic $Ga_{0.56}In_{0.44}P$ host. Figure 7 presents AFM and PL data from an InP/$Ga_{0.56}In_{0.44}P$ 10-period QD/host structure, with PL comparison to the lattice-matched case. The QD layers were produced using a deposition of 4.2 ML InP and a terminal QD capping layer was grown to enable topographical analysis. No intentional strain-compensation was applied. FWHM (full-width at half-max) is noted for each QD PL emission peak and substrate and host emission peaks are also labeled. We see here that, while the QDs are still basically square-pack ordered and

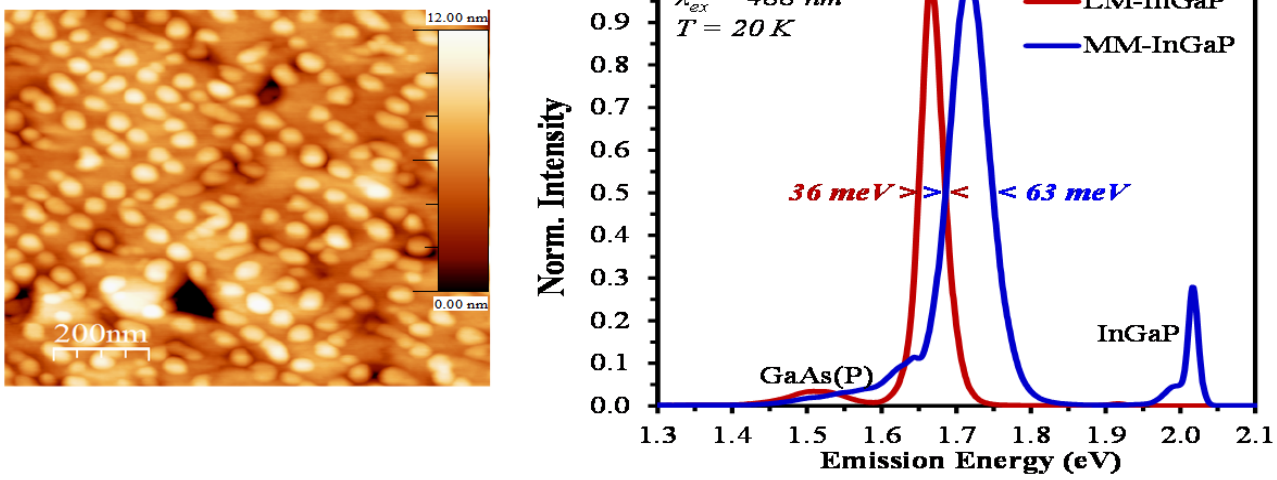

(a) **(b)**

Figure 7. (a) AFM image and (b) low-temperature PL spectra for a 10-period InP/ $Ga_{0.56}In_{0.44}P$ QD/host multilayer structure; PL from a similar InP/ $Ga_{0.51}In_{0.49}P$ structure is also shown.

about the same size, the high degree of long-range order has been effectively lost, and definite pitting is occurring, suggesting that the metamorphic $Ga_{0.56}In_{0.44}P$ host material is becoming unstable. This is likely due to the fact that there is some residual strain remaining in the metamorphic buffer and/or initial host layer, exacerbated by the higher QD/host misfit (4.2% vs. 3.8%), but should be controllable with very careful internal lattice-matching and strain compensation. The PL comparison shows a slightly stronger blue shift for the metamorphic case, even though the QDs are about the same size and are InP in both cases. This could be due to tighter quantum confinement coming from the higher barrier (wider band gap) or possibly some Ga in-diffusion into the QDs; the higher Ga-content metamorphic host material could lead to a slightly different diffusion equilibrium compared leading to the lattice-matched case.

4.4 InAs QDs with GaAs Host for Comparison to OMVPE-Grown Structures

Since InAs/GaAs QD growth by MBE has been well-studied, the main purpose of this task was to develop in-house capabilities to produce InAs/GaAs QD/host structures equivalent to those made by the Hubbard group (RIT) via OMVPE for comparison via defect spectroscopy (DLTS). This ended up being a relatively time-consuming undertaking, given the number of components involved. Initial work focused on development of InAs QD nucleation and growth conditions to yield QD sizes, uniformity, and density approximately equal to that of the Hubbard structures. Following achievement of this, we moved on to encapsulation studies, and then ultimately to the growth of multilayer samples. The latter also required the development of strained, low-temperature GaP growth for strain-balancing. Figure 8 presents AFM from our first attempt at a 10-period, strain-balanced multilayer targeting the structure used by the Hubbard group for their QD-embedded solar cells. Although additional optimization is clearly needed in order to yield the target QD uniformity and density, followed by optimization of the strain-balancing layers (using XRD), we can see that we did succeed in producing a structure that was able to maintain strain conditions amenable to QD formation throughout; we were unable to achieve this for multilayer samples without the strain-compensation layers. Unfortunately, due to the sizable scope of the development and optimization of the MBE-grown InAs/GaAs QD structure, before we were able to work on significant optimization our MBE system needed to go down for

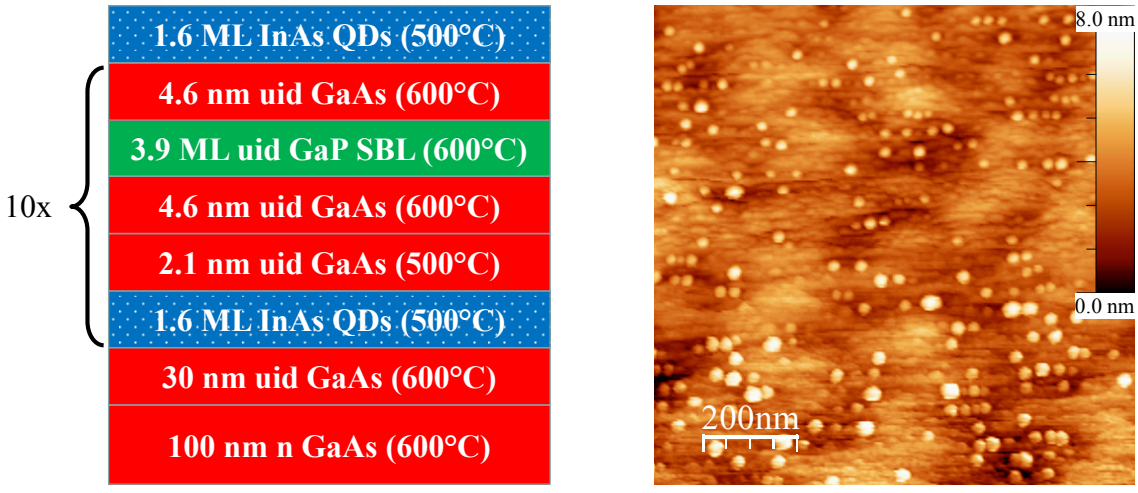

(a) **(b)**

Figure 8. (a) Diagram and (b) AFM image of a 10-period multilayer InAs/GaAs QD/host structure, with thin GaP strain-balancing layers (SBL).

maintenance, which ended up lasting beyond the end date of this project. We nonetheless intend to complete this interesting phase of the project as soon as possible.

4.5 Defect spectroscopy of III-V QD materials

The goal of this task was to perform DLTS measurements on the QD-embedded III-V materials produced, with a particular focus on comparing MBE and metal-organic chemical vapor deposition (MOCVD)/OMVPE grown InAs/GaAs structures. As discussed in the previous section, we have been so far unable to perform DLTS measurements on MBE-grown samples. However, we have performed measurements on OMVPE-grown samples shared with us by the Hubbard group. We received, and have characterized, two samples: a baseline *p-i-n* GaAs solar cell structure and an InAs QD-embedded *p-i-n* GaAs solar cell structure (10-period multilayer). By performing these measurements using a careful depth-resolved approach, making using of the capacitance depletion edge, we have been able to deconvolve the trap population due to the inclusion of the QDs from the traps within the plain epitaxial GaAs.

Figure 9 displays measured DLTS data from the OMVPE-grown QD and baseline samples received from the Hubbard group. A few different comparisons are made between the sample to elucidate the location and cause of the trap populations. In all cases only one definite trap is observed at E_C – 0.69 eV (electron trap, since "*i*-layer" is slightly *n*-type), making it almost exactly mid-gap; the small capture cross-section (~6.8×10^{-16} cm^{-3}) suggests the trap is some kind of point defect, making it consistent with the standard "EL2" trap family typically seen in GaAs. What is particularly interesting, and important, is that the region containing the QDs possesses a much greater density of these traps than the pure GaAs baseline material (>> 72x higher local density based on total integrated density), possibly due to the high localized strain fields. It is also possible that the GaP strain-balancing layers play some role, since GaP is known to possess high densities of a wide range of traps. The region above the QDs is found to possess a low trap density, suggesting that the inclusion of the QDs does not detrimentally impact the subsequent material quality, most likely due in part to the effective strain-balancing. Nonetheless, the substantial increase in trap density around the QDs is of concern for performance of such devices and the potential for non-radiative recombination. It will be interesting to see how the MBE-grown InAs/GaAs system compares.

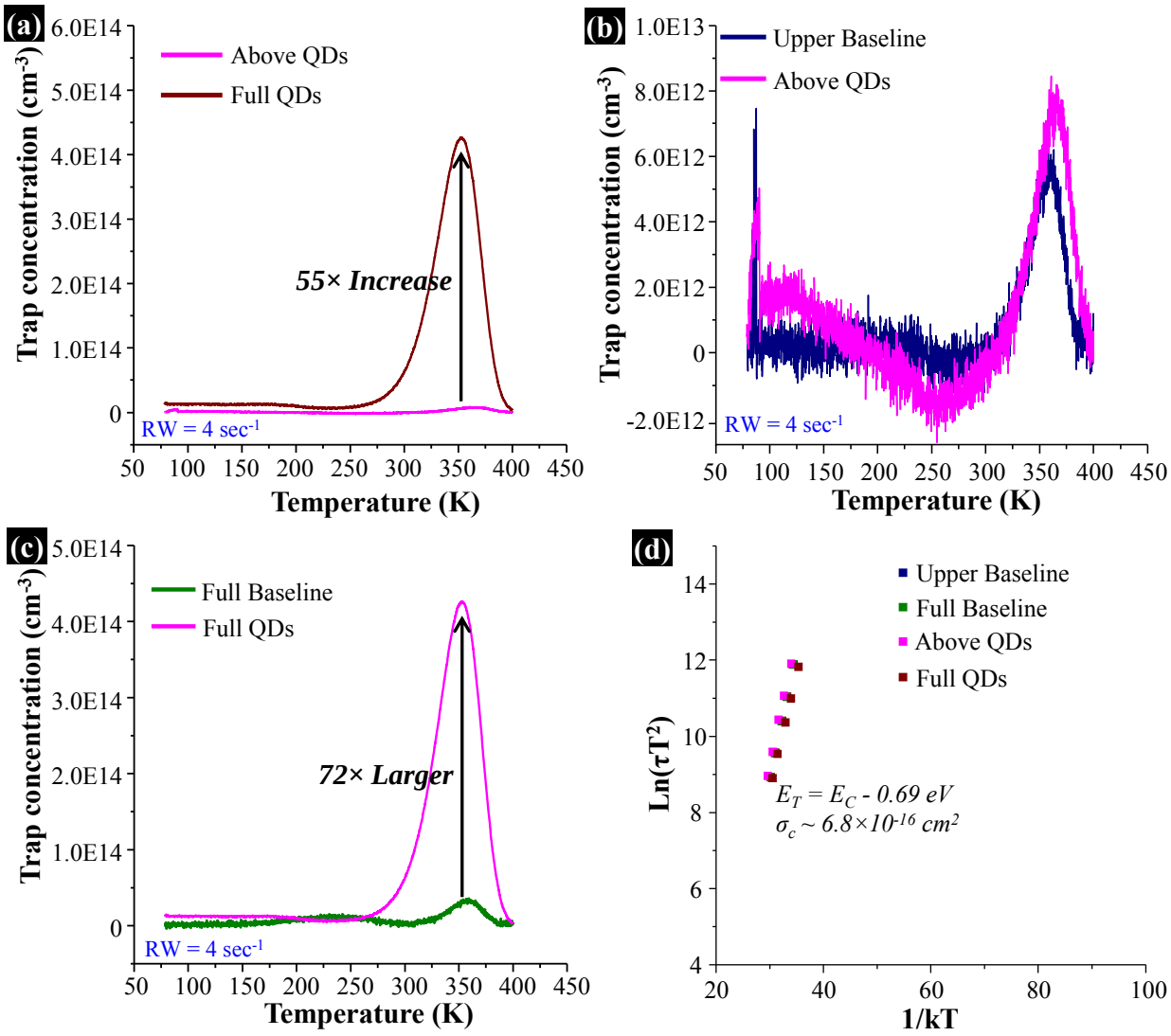

Figure 9. DLTS measurements made on baseline GaAs and InAs QD-embedded GaAs *p-i-n* solar cells, with comparisons of: (a) between the region above the QDs and the full QD sample; (b) between the upper region of the baseline and region above the QDs; and (c) between the full baseline and the full QD. (d) Arrhenius plot of the measured trap levels showing them all to be identical.

5 CONCLUSIONS

5.1 GaInAs QDs on/in GaAsP Host by MBE

The comparison between equal-misfit QD/host systems based on GaAs and metamorphic $GaAs_{0.90}P_{0.10}$ substrates showed an interesting difference in achieved QD morphologies. While the "lattice-matched" GaAs-based system showed a high degree of long-range order, the metamorphic $GaAs_{0.90}P_{0.10}$-based samples did not, although areas of short-range order were visible. It is possible that a higher degree of ordering could be achieved in the metamorphic samples if a larger number of multilayer periods were used. The comparison made here pitted a 60x GaAs-based samples against a 20x $GaAs_{0.90}P_{0.10}$-based sample, based upon QD uniformity, but it is worth noting that the ordering of the GaAs-based samples from the previous work were found to be less ordered at lower numbers of periods (20x, 40x). Both systems showed good QD size uniformity, but the metamorphic QDs appeared to yield a higher degree of uniformity at a lower number of multilayer periods. Additionally, the metamorphic QDs were found to be smaller and denser, resulting in a larger blue-shift in the PL spectra.

Because the lattice-mismatch between the QDs and the host materials studied here were nominally equal, these results suggest that there is some impact due to the use of a metamorphic host. It is possible that the source of these differences is related to the presence of strain fields in the metamorphic material, even though it is effectively relaxed and the residual dislocation density is approximately orders of magnitude lower than the QD density. Another possibility is with respect to vicinality, where the metamorphic substrates exhibits an undulating surface due to the existence of cross-hatch resulting from dislocation glide, which produces regions of increased effective off-cut. Tensile-graded substrates tend to be very smooth compared to compressive-graded substrates, but they do still possess cross-hatch; previous work in our group did indicate a difference between QD growth on compressive vs. tensile substrates, but the issue has not been sufficiently studied to draw any strong conclusions. Additionally, such an effect might be expected to showed long-range non-uniformity on the order of the cross-hatch dimension. While we did not observe such non-uniformity, are more in-depth, quantitative analysis may be needed to draw any firm conclusions.

The literature contains a range of conflicting conclusions on the effect of metamorphic grading and substrate vicinality. The smaller and higher density QDs found for the metamorphic $Ga_{0.55}In_{0.45}As/GaAs_{0.90}P_{0.10}$ case is most consistent with reports of increasing critical thickness for increasing substrate offcut, which leads to the production of smaller, higher density QDs [11]. Regardless the cause of the difference in QD morphology, it is evident that the use of metamorphic substrates provides not only better control over the QD/host electronic structure, but also provides an additional parameter for control over QD size and density beyond what misfit and deposition conditions can provide, which could be useful in the future development of IBSC devices.

5.2 InAs QDs on/in GaInP Host by MBE

The result obtained for InAs QDs on lattice-matched $Ga_{0.51}In_{0.49}P$ host materials were very interesting, with the massive non-uniformity in QD morphology and the resultant detrimental

apparent decomposition of the phase unstable matrix upon encapsulation. The source of this substantial non-uniformity is not definitively known. However, it is interesting to note that nearly identical results were achieved by the Hubbard/Forbes group from RIT/NASA-Glenn for InAs QDs grown on $Ga_{0.51}In_{0.49}P$ via OMVPE [12]. Because the volume of the resultant dots/blobs is significantly higher than the volume of InAs actually deposited, they suggest that the issue is due to In diffusion out of the $Ga_{0.51}In_{0.49}P$ surface (effectively a near-infinite source of the element) and into the InAs dots, thereby ultimately increasing the amount of In being incorporated into the QDs. Indeed, this explanation appears to be consistent with our results, as well. It is possible that there is also some impact due to As-P anion exchange, which would could cause issues related to the actual interfacial composition and resultant strain state, but this effect, if in existence, appears to be smaller than the In accumulation, especially since no deleterious problems of this sort are observed when growing InAs dots on GaAsP surfaces, where As-P exchange is also possible. However, the In accumulation hypothesis does not seem to bear out in and of itself when considering InP QDs with $Ga_{0.51}In_{0.49}P$ hosts, where the dots form uniformly and controllable. Therefore, it does appears though there actually is some effect related to the presence of As, such as possibly a larger driving force for the In diffusion, although the lower formation energy for InAs versus InP does not support such a thermodynamic argument. Most like it is a combination of multiple issues that is at play, with additional issues related to different degrees of interfacial strain and bond lengths, making elucidation difficult.

Due to the difficulty of controllably and reliably nucleating uniform InAs QDs, and the extreme sensitivity of the $Ga_{0.51}In_{0.49}P$ encapsulation, even when nominally lattice-matched to the GaAs substrate, attention to this particular task was put on hold in order to concentrate on other tasks. Additionally, it is worth noting that the goal of this task was to utilize the metamorphic $Ga_{0.56}In_{0.44}P$ as a ~2.0 eV host material. While the instability issues of the GaInP alloy system appear as though this will be a difficult task, another 2.0 eV direct gap composition, without the need for high Al concentrations, is nonetheless available in the GaAsP alloy system at $GaAs_{0.52}P_{0.48}$, which is accessible via the extension of the $GaAs_yP_{1-y}$ tensile-graded buffer. Because GaAsP exhibits no phase instability at all, this is likely to be a more reliable target for QD inclusion.

5.3 InP QDs on/in GaInP Host

Within the context of this project, and the tasks discussed above, a particularly interesting result was the lack of non-uniformity issues encountered in the InP/$Ga_{0.51}In_{0.49}P$ effort, as compared to the relatively "disastrous" results when using InAs QDs. Indeed, uniformity and long-range order was readily achievable in the "lattice-matched" InP/$Ga_{0.51}In_{0.49}P$, and while the metamorphic InP/$Ga_{0.56}In_{0.44}P$ experiments indicated a slightly higher level of difficult, it appears as though careful control over residual strain and strain-balancing should serve to suppress phase decomposition. Unfortunately, InP does not possess the right band gap to be useful in an IBSC configuration (which was why it was not an initial target for this project). Therefore, it appears that it will be impossible to avoid using an As-containing QD material, in which case the same issues encountered with InAs can be expected. There have been some reports in the literature of getting around this problem by using a thin GaAs interfacial layer between the $Ga_{0.51}In_{0.49}P$ and the InAs QDs, enabling uniform nucleation and growth [13]. However, such a growth structure complications the electronic structure of the system and would probably be best avoided. It may

be possible, however, to utilize a similar structure, but replace the GaAs with GaP, allowing it to serve as both QD nucleation enabler and strain-balancing layer. Another possibility is to dispense entirely with GaInP as host material and move to wider gap GaAsP, which eliminates all issues relating to In accumulation and phase instability. Both approaches are of interest for future (and current) studies.

5.4 Comparison of MBE- and OMVPE-Grown InAs/GaAs QD/Host Structures

While interesting results were obtained in this effort, it is as of yet incomplete. The DLTS of the OMVPE-grown InAs/GaAs QD/host solar cell structures provided by the Hubbard group provided valuable insight into the defects produced by the inclusion of QDs into the solar cell host material. Most notably is the nearly two order of magnitude of increase in mid-gap trap density in the QD-containing region, suggesting the potential for significant non-radiative recombination in this area. It is quite possible that this effect is a significant component of the reduced open-circuit voltage (V_{OC}) typically observed in QD-embedded solar cells, and may also serve to reduce the short-circuit current (J_{SC}) gains that might be expected from the inclusion of the QDs. The role of the GaP strain-balancing layers also cannot be ruled out, since this material is known, through both previous reports and our own recent work, to possess large densities of a range of traps. It will thus be interesting to observe if and how MBE-grown material differs, either in density and/or type of traps. It would also be of interest to compare with structures that do not possess strain-balancing layers of any sort.

REFERENCES

1. A. B. Cornfeld, D. Aiken, B. Cho, A. V. Ley, P. Sharps, M. Stan and T. Varghese, "Development of a Four Sub-Cell Inverted Metamorphic Multi-Junction (IMM) High Efficiency AM0 Solar Cell," *35th IEEE Photovoltaic Specialists Conference*, 105 (2010), Honolulu, HI.

2. C. D. Cress, S. M. Hubbard, B. J. Landi, R. P. Raffaelle and D. M. Wilt, "Quantum dot solar cell tolerance to alpha-particle irradiation," *Applied Physics Letters **91**(18)*, 183108 (2007).

3. C. G. Bailey, D. V. Forbes, R. P. Raffaelle and S. M. Hubbard, "Near 1 V open circuit voltage InAs/GaAs quantum dot solar cells," *Applied Physics Letters **98**(16)*, 163105 (2011).

4. A. Marti, L. Cuadra and A. Luque, "Quasi-drift diffusion model for the quantum dot intermediate band solar cell," *IEEE Transactions on Electron Devices **49**(9)*, 1632 (2002).

5. C. D. Cress, S. J. Polly, S. M. Hubbard, R. P. Raffaelle and R. J. Walters, "Demonstration of a *nipi*-diode photovoltaic," *Progress in Photovoltaics: Research and Applications **19**(5)*, 552 (2011).

6. J. Grandal, T. J. Grassman, A. M. Carlin, M. R. Brenner, B. Galiana, J. A. Carlin, L.-M. Yang, M. J. Mills and S. A. Ringel, "Growth and characterization of InGaAs quantum dots on metamorphic GaAsP templates by molecular beam epitaxy," *38th IEEE Photovoltaic Specialists Conference*, 001783 (2012), Columbus, OH.

7. L. M. McGill, E. A. Fitzgerald, A. Y. Kim, J. W. Huang, S. S. Yi, P. N. Grillot and S. A. Stockman, "Microstructural defects in metalorganic vapor phase epitaxy of relaxed, graded InGaP: Branch defect origins and engineering," *Journal of Vacuum Science & Technology B: Microelectronics and Nanometer Structures **22**(4)* (2004).

8. N. J. Quitoriano and E. A. Fitzgerald, "Relaxed, high-quality InP on GaAs by using InGaAs and InGaP graded buffers to avoid phase separation," *Journal of Applied Physics **102**(3)*, 033511 (2007).

9. J. R. R. Bortoleto, H. R. Gutierrez, M. A. Cotta, J. Bettini, L. P. Cardoso and M. M. G. de Carvalho, "Spatial ordering in InP/InGaP nanostructures," *Applied Physics Letters **82**(20)*, 3523 (2003).

10. C. Pryor, M. E. Pistol and L. Samuelson, "Electronic structure of strained InP/Ga_{0.51}In_{0.49}P quantum dots," *Physical Review B **56**(16)*, 10404 (1997).

11. S. M. Hubbard, A. Podell, C. Mackos, S. Polly, C. G. Bailey and D. V. Forbes, "Effect of vicinal substrates on the growth and device performance of quantum dot solar cells," *Solar Energy Materials and Solar Cells **108**(0)*, 256 (2013).

12. D. V. Forbes, A. M. Podell, M. A. Slocum, S. J. Polly and S. M. Hubbard, "OMVPE of InAs quantum dots on an InGaP surface," *Materials Science in Semiconductor Processing* ***16****(4)*, 1148 (2013).

13. H. Amanai, S. Nagao and H. Sakaki, "Growth and temperature characteristic of self-assembled InAs-QD on GaInP," *Journal Of Crystal Growth* ***251****(1–4)*, 223 (2003).

LIST OF ACRONYMS, ABBREVIATIONS, AND SYMBOLS

Acronym/Abbreviation	Description
AFM	atomic force microscopy
CL	cathodoluminescence
DLTS	deep level transient spectroscopy
FWHM	full-width at half-max
IBSC	intermediate band solar cell
MBE	molecular beam epitaxy
MJ	multijunction
MOCVD	metal-organic chemical vapor deposition
OMVPE	organometallic vapor phase epitaxy
PL	photoluminescence
PV	photovoltaic(s)
QD	quantum dot
RHEED	reflection high energy electron diffraction
RIT	Rochester Institute of Technology
RSM	reciprocal space map
SBL	strain-balancing layer
SOW	statement of work
TDD	threading dislocation density
UHV	ultra-high vacuum
XRD	X-ray diffraction

Symbol/Unit	Description
E_C	conduction band energy
E_g	band gap
E_T	trap energy
J_{SC}	short-circuit current density
ML	monolayer
N_D	donor impurity density
σ_c	capture cross section
T	temperature
V_{OC}	open-circuit voltage

DISTRIBUTION LIST

DTIC/OCP
8725 John J. Kingman Rd, Suite 0944
Ft Belvoir, VA 22060-6218 1 cy

AFRL/RVIL
Kirtland AFB, NM 87117-5776 2 cys

Official Record Copy
AFRL/RVSV/David Wilt 1 cy

(This page intentionally left blank)